Hydrologic Variability and Uncertainty Analysis through Hydroclimatic Teleconnection

D. Nagesh Kumar

Department of Civil Engineering
Indian Institute of Science
Bangalore – 560012

URL: http://www.civil.iisc.ernet.in/~nagesh

Outline

- **Introduction**
  - El Niño-Southern Oscillation (ENSO)
  - Equatorial Indian Ocean Oscillation (EQUINOO)
- **Hydroclimatic teleconnection for Indian subcontinent**
  - Bayesian dynamic modeling of Indian summer monsoon rainfall
  - Copula: Nonparametric scale-free dependence
- **Hydroclimatic teleconnection at basin-scale**
  - Variability of basin-scale hydrologic variables
  - Forecast of monthly streamflow
- **Optimal reservoir operation with climate inputs**
- **Conclusions**

Introduction

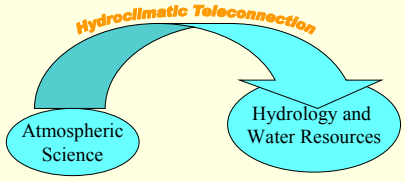

Hydroclimatic Teleconnection: The significant association between hydrologic events and large-scale atmospheric circulation patterns, which are widely separated across the globe, is referred as 'hydroclimatic teleconnection'.

Natural variability of hydrologic variables and hydroclimatic teleconnection

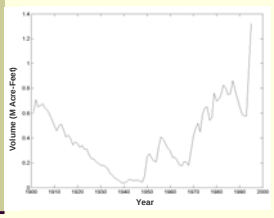

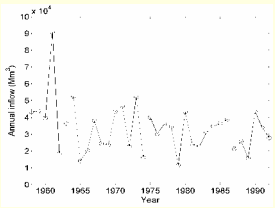

- It is recently being established that temporal structure of hydrologic time series is significantly forced by large-scale atmospheric circulation patterns through **hydroclimatic teleconnection** (Jain and Lall, 2001)

Major Issues/Challenges

- Dynamic nature of cause-effect relationship between hydrologic time series and large-scale circulation is to be captured.
- Uncertainty associated with the prediction to be addressed
- Consideration of nonstationarity in time series, expected under climate change scenario.
- 'Large-Scale' to 'Basin-Scale': It is necessary to establish the link.
- Being most essential for Hydrology and Water Resources, responses of 'basin-scale' hydrologic variables to 'large-scale' atmospheric circulation will be investigated
- Use of such relationship with a goal to improve the prediction performance of hydrologic time series.

El Niño-Southern Oscillation (ENSO)

- El Niño-Southern Oscillation (ENSO) is the coupled Ocean-atmosphere mode of tropical Pacific Ocean (Cane, 1992)
- Attempts were made to forecast hydrologic variables, like rainfall, streamflow, etc., using ENSO information all over the world (Dracup and Kahya, 1994; Eltahir, 1996; Jain and Lall, 2001).

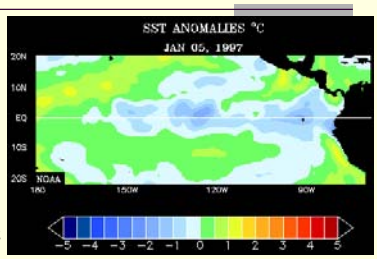

Source: NOAA

El Niño-Southern Oscillation (ENSO)

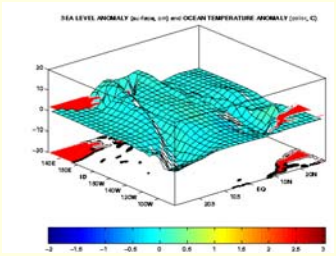

Source: NOAA

El Niño-Southern Oscillation (ENSO)

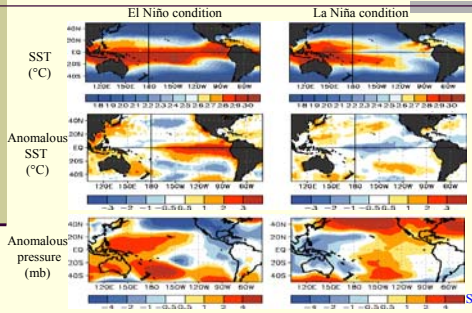

Source: NOAA

Change in Atmospheric Circulation

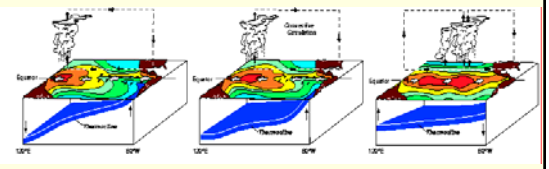

La Niña condition Normal condition El Niño condition

Source: NOAA

Impact of El Niño

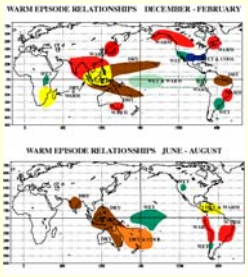

Rainfall defiencies
Africa, Indian Subcontinent, Northern China, Australia, Northern South America and the Caribbean

Low river discharge
Nile (Egypt), Senegal (Senegal), Orange (South Africa), Krishna (India), Murray-Darling (Australia) and Amazon (Brazil) river system

Surplus rainfall
Western Europe, Eastern Africa, Western Cape of South Africa, Gulf regions of the united states and northern Mexico and central Chile.

Sources: NOAA
Allan et al., 1996

Impact of La Niña

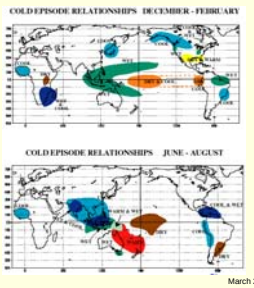

Increased Rainfall
Africa, Indian Subcontinent, Northern China, Australia, Northeastern South America

High River Discharge
Nile, Senegal, Orange, Krishna, Murray-Darling and Amazon

Enhanced Monsoonal/ Tropical-linked summer rainfall
Southern Africa and India, and prominent cloud band influences lead to rainfall surplus regions over southern Australia and southern Africa

Sources: NOAA
Allan et al., 1996

Niño Regions

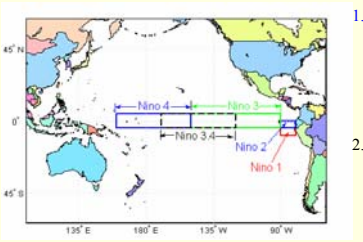

1. Niño 3.4 sea surface temperature anomaly (Niño 3.4 SSTA) is best correlated with Indian summer monsoon rainfall (ISMR)
2. Three months running mean of Niño 3.4 SSTA is known as Oceanic Nino Index (ONI)

Indian Ocean Dipole (IOD) mode

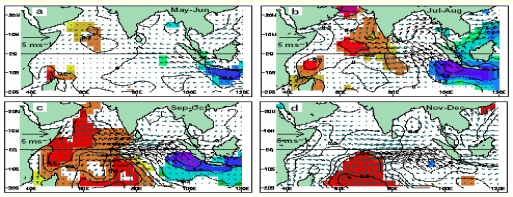

A pattern of internal variability with anomalously low sea surface temperatures near Sumatra and high sea surface temperatures in the western Indian Ocean, with accompanying wind and precipitation anomalies

Source: *Saji et al., Nature*, 1999

Equatorial Indian Ocean Oscillation (EQUINOO)

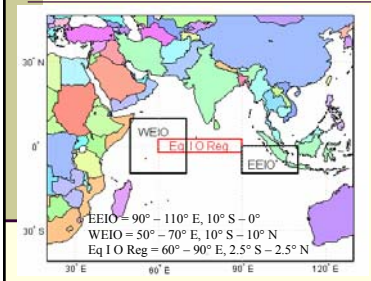

EEIO = 90° – 110° E, 10° S – 0°
WEIO = 50° – 70° E, 10° S – 10° N
Eq I O Reg = 60° – 90° E, 2.5° S – 2.5° N

- Atmospheric component of Indian Ocean Dipole (IOD) Mode is known as EQUINOO.
- EQUINOO is defined as the oscillation between two opposite states of convection over EEIO and WEIO.
- Equatorial zonal wind index (EQWIN) is considered as a measure of this which is the negative of the anomaly of zonal wind at Eq. I O Reg.

Impact of IOD/ EQUINOO

IOD plays an important role as a modulator of the Indian summer monsoon rainfall (ISMR)

Whenever the ENSO-ISMR correlation is low (high), the IOD-ISMR correlation is high (low) (Ashok et al., 2001)

Indian summer monsoon rainfall is associated not only with ENSO, but also with EQUINOO (Gadgil et al., 2003)

Examples:	Year	ENSO	EQUINOO	ISMR
	1983,1994	El Niño	+ve	excess
	1979, 1985	La Niña	-ve	drought
	2002	El Niño	-ve	severe drought

Composite Index between ENSO and EQUINOO has more power to predict ISMR (Gadgil et al., 2004)

Bayesian Dynamic Linear Model (BDLM)

Important Features

- Dynamic nature of the model helps to capture the time varying relationship between climate information and hydrologic variables
- Allows incorporation of exogenous inputs
- Relaxation of stationarity assumption
- Allowance for on-line external intervention
- Probabilistic Forecast

BDLM for monthly summer monsoon rainfall over India*

Observation Equation: $Y_{i,j} = F_{i,j}^T \Theta_{i,j} + v_{i,j} \qquad v_{i,j} \sim N[0, V]$

where $F_{i,j} = \begin{bmatrix} 1 \\ f * EN_{i,j-\kappa} \\ (1-f) * EQ_{i,j-\lambda} \end{bmatrix}$ and $\Theta_{i,j} = \begin{bmatrix} \overline{Y_j} \\ \theta_{i,j}^{en} \\ \theta_{i,j}^{eq} \end{bmatrix}$

System Equation: $\theta_{i,j} = \theta_{i,j-1} + \omega_{i,j}$ for $\forall\, i$ and $j = 2,..,12$

$\theta_{i,j} = \theta_{i-1,12} + \omega_{i,j}$ for $\forall i$ and $j = 1$

where $\omega_{i,j} \sim T_n[0, W_{i,j}]$ and $n = (i-1)*12 + j - 1$

Initial Information $(\theta_{1,0} / D_{1,0}) \sim T_0[m_{1,0}, C_{1,0}]$ and $(\phi / D_{1,0}) \sim G[n_{1,0}/2,\ d_{1,0}/2]$

where $\phi = V^{-1}$

*** Journal of Geophysical Research – Atmospheres, AGU, 2006**

BDLM for summer monsoon rainfall over India...contd.

At Time step $(i, j\text{-}1)$ $(\theta_{i,j-1} / D_{i,j-1}) \sim T_n[m_{i,j-1}, C_{i,j-1}]$ and $(\phi / D_{i,j-1}) \sim G[n_{i,j-1}/2, d_{i,j-1}/2]$

Prior distribution for $\theta_{i,j}$ $(\theta_{i,j} / D_{i,j-1}) \sim T_n[m_{i,j-1}, R_{i,j}]$ where $R_{i,j} = C_{i,j-1} + W_{i,j}$

$W_{i,j}$ is the system evolution variance. It is practically difficult to assign the sequence of evolution variance $\{W_{i,j}\}$ without relating it to some previous known variance.

$$R_{i,j} = C_{i,j-1} / \delta \qquad (0 < \delta \le 1)$$

Thus $W_{i,j} = C_{i,j-1}(\delta^{-1} - 1)$

BDLM for summer monsoon rainfall over India...contd.

One-step ahead forecast distribution $\left(Y_{i,j} / D_{i,j-1}\right) \sim T_n\left[F_{i,j}, Q_{i,j}\right]$

where $F_{i,j} = \overline{Y}_j + EN_{i,j-\kappa} * f * m_{i,j-1}^{en} + EQ_{i,j-\lambda} * (1-f) * m_{i,j-1}^{eq}$

$$Q_{i,j} = \left(EN_{i,j-\kappa} * f\right)^2 * R_{i,j}^{en} + \left\{EQ_{i,j-\lambda} * (1-f)\right\}^2 * R_{i,j}^{eq} + S_{i,j-1}$$

$$S_{i,j-1} = \frac{d_{i,j-1}}{n_{i,j-1}}$$

Posterior distribution for $\theta_{i,j}$ $\left(\theta_{i,j} / D_{i,j}\right) \sim T_n\left[m_{i,j}, C_{i,j}\right]$

where $m_{i,j} = m_{i,j-1} + A_{i,j} e_{i,j}$ $C_{i,j} = R_{i,j} S_{i,j} / Q_{i,j}$ $S_{i,j} = d_{i,j} / n_{i,j}$

$e_{i,j} = Y_{i,j} - f_{i,j}$ $A_{i,j}^{en} = EN_{i,j-\kappa} * f * R_{i,j} / Q_{i,j}$ $A_{i,j}^{eq} = EQ_{i,j-\lambda} * (1-f) * R_{i,j} / Q_{i,j}$

BDLM for summer monsoon rainfall over India...contd.

Distributional form of scale parameter ϕ at time step (i, j)

$$\left(\phi / D_{i,j}\right) \sim G\left[n_{i,j} / 2, d_{i,j} / 2\right]$$

where $n_{i,j} = n_{i,j-1} + 1 \quad d_{i,j} = d_{i,j-1} + S_{i,j-1} e_{i,j}^2 / Q_{i,j}$

Data

Large Scale circulation Information: ENSO index and EQUINOO index

Target Variable: Monthly rainfall over India

Model Calibration Period : 1958 – 1985
Model Testing Period : 1986 – 2003

Model Performance during testing period 1986 – 2003

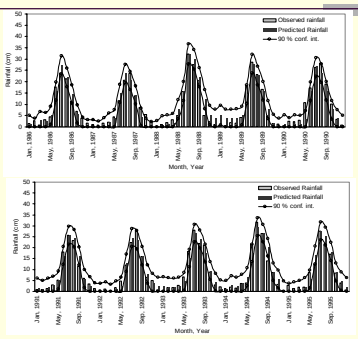

Model Performance during testing period 1986 – 2003

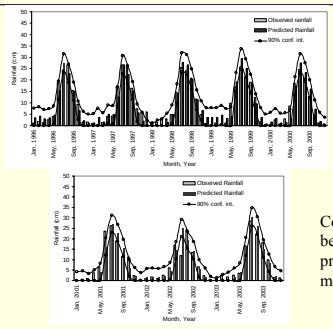

Correlation coefficient between observed and predicted rainfall during monsoon months = 0.82

Model Performance during testing period 1986 – 2003

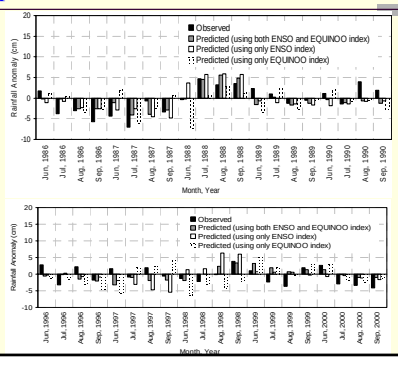

Summary

- Efficacy of the BDLM to capture the dynamic relationship between monthly rainfall anomaly and circulation indices is established.
- Predictions of uncertain future values are available in a distributional form.
- Concurrent influence of ENSO and EQUINOO index on monthly rainfall variation is established.
- Unusual recent experiences are satisfactorily explained by this approach, for instance, 1997, 2002 etc.
- Both ENSO and EQUINOO have significant influence on monthly Indian summer monsoon rainfall.

Scale-free dependence between hydroclimatic variables using Copula

Copula

A copula is a function that joins or couples multiple distribution functions to their one-dimensional marginal distribution functions.

Let X and Y be a pair of 'Random Variables' with cdf as $F_X(x)$ and $G_Y(y)$. Also let their joint cdf as $H_{X,Y}(x,y)$.

Each pair (x,y) leads to a point in the unit square [0,1]x[0,1]. And this ordered pair in turn corresponds to a number $H_{X,Y}(x,y)$ in [0,1].

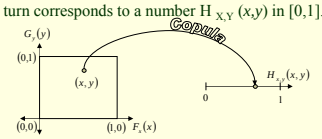

This correspondence is indeed a function. This function is known as Copula

Introduction to Copula

Sklar's Theorem

Let, $H_{X,Y}(x,y)$ is a Joint distribution function with margins $F_X(x)$ and $G_Y(y)$. Then there exists a copula C such that for all x, y in $\bar{R}$,

$$H_{X,Y}(x, y) = C(F_X(x), G_Y(y))$$

If F and G are continuous, then C is unique; otherwise, C is uniquely determined on RanF x RanG.

Conversely, if C is a copula and $F_X(x)$ and $G_Y(y)$ are CDFs, then

$$H_{X,Y}(x, y) = C(F_X(x), G_Y(y))$$

is the joint CDF with margins $F_X(x)$ and $G_Y(y)$)

Archimedean Copula

A copula that can be expressed in terms of

$$C(u,v) = \varphi^{[-1]}(\varphi(u) + \varphi(v))$$

known as 'Archimedean copula', where φ is a strictly decreasing, continuous function and φ is known as generator of Copula

$\varphi^{[-1]}$ is known as 'pseudo inverse' and defined as

$$\varphi^{[-1]}(t) = \begin{cases} \varphi^{-1}(t), & 0 \le t \le \varphi(0) \\ 0, & \varphi(0) \le t \le \infty \end{cases}$$

Expression for Kendall's τ reduced to $\tau = 1 + 4\int_0^1 \frac{\varphi(u)}{\varphi'(u)} du$

Archimedean Copula

	$C_\theta(u,v)$	$\varphi_\theta(t)$	$\theta \in$
Clayton	$\left[\max\left(u^{-\theta}+v^{-\theta}-1,\,0\right)\right]^{-1/\theta}$	$\frac{1}{\theta}\left(t^{-\theta}-1\right)$	$[1,\infty)\setminus\{0\}$
Frank	$-\frac{1}{\theta}\ln\left(1+\frac{\left(e^{-\theta u}-1\right)\left(e^{-\theta v}-1\right)}{e^{-\theta}-1}\right)$	$-\ln\left(\frac{e^{-\theta t}-1}{e^{-\theta}-1}\right)$	$(-\infty,\infty)\setminus\{0\}$
Ali-Mikhail-Haq	$\frac{uv}{1-\theta(1-u)(1-v)}$	$\ln\frac{1-\theta(1-t)}{t}$	$[-1,1)$
Gumbel-Hougaard	$\exp\left(-\left[(-\ln u)^\theta+(-\ln v)^\theta\right]^{1/\theta}\right)$	$(-\ln t)^\theta$	$[1,\infty)$

Copula-based method to capture scale-free dependence pattern

Nonparametric estimate of probability density

Kernel density estimator is most popular for estimation of nonparametric density

$$\hat{f}(x) = \frac{1}{n}\sum_{i=1}^{n} K_h(x - X_i)$$

where $K_h(z) = \frac{1}{h}Kr\left(\frac{z}{h}\right)$

kernel function: Naïve, Normal, Epanechnikov

Smoothing parameter

Copula-based method to capture scale-free dependence pattern

Step 1

Sample estimate of Kendall's Tau

$$\hat{\tau} = P\left[(x_i - x_j)(y_i - y_j) > 0\right] - P\left[(x_i - x_j)(y_i - y_j) < 0\right] = \frac{c}{{}^nC_2} - \frac{d}{{}^nC_2} = \frac{c-d}{{}^nC_2}$$

Step 2

Sample estimate of Kendall's Tau is plugged in the following equation

$$\tau = 1 + 4\int_0^1 \frac{\varphi_\theta(u)}{\varphi'_\theta(u)} du$$

Estimate of θ is available for a particular Copula

Copula-based method to capture scale-free dependence pattern

Step 2 ..contd

Simulation with a particular Copula (Genest and MacKay, 1986b)

a) $\varphi^{[-1]}(\bullet)$, $\varphi'(\bullet)$ and $\varphi'^{(-1)}(\bullet)$ are obtained

b) $U = [\sim Un(0,1)]$; $T = [\sim Un(0,1)]$

c) $S = \varphi'(U)/T$; $W = \varphi'^{(-1)}(S)$

d) $V = \varphi^{[-1]}(\varphi(W) - \varphi(U))$

e) The pair U and V are the simulated pair, preserving the dependence structure

f) U and V are then transformed by inverse cumulative distribution function

Copula-based method to capture scale-free dependence pattern

Step 3

Selection of the most appropriate copula (Genest and Rivest, 1993; Zhang and Singh, 2006)

Parametric $K(z) = z - \frac{\varphi(z)}{\varphi'(z^+)}$

Nonparametric $K_n(z) =$ the fraction of $z_i \le z$

where $z_i = \frac{\text{Number of } (x_j, y_j) \text{ such that } x_j < x_i \text{ and } y_j < y_i}{(N-1)}$ $\quad i = 1,\ldots,N$ $\quad j = 1,\ldots,N$ $\quad j \ne i$

A scatter plot between $K(z)$ and $K_n(z)$ is prepared

The better the fit, the closer the corresponding scatter to a 45° line through origin

Lowest value of sum of square errors (SSE) from the 45° line through origin

Copula-based method to capture scale-free dependence pattern

Step 4

After selecting the best copula, a large number (~10^4) of jointly distributed values are numerically simulated. These values are back transformed by using the corresponding non-parametrically estimated cumulative probability density.

Step 5

Keeping any observed value of climate precursors at the centre, a sufficiently 'small' window around it, is selected. Statistical properties of the simulated values of the response variable, lying within this window, are investigated through box plot. The median of these values is used as a prediction, corresponding to the observed value of the climate precursor. The interquartile range (75th percentile – 25th percentile) of these values indicates the associated uncertainty

Dependence of ISMR on ENSO and EQUINOO

- Target Time series → Monthly all India rainfall
- Exogenous Input → Combined index of ENSO and EQUINOO

Combined index $CI_{i,j} = c_1 EN_{i,j-\kappa} + c_2 EQ_{i,j-\lambda}$

where $c_1 = 0.61$

$c_1 = 0.29$

$\kappa = 2$

$\lambda = 1$

Simulation with different copulas

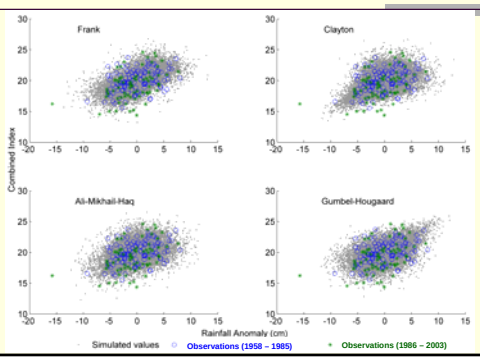

Selection of an appropriate Copula and corresponding joint density

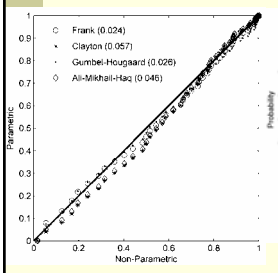

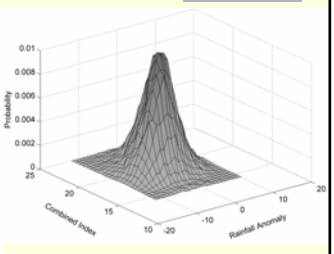

Comparison between observed and predicted rainfall

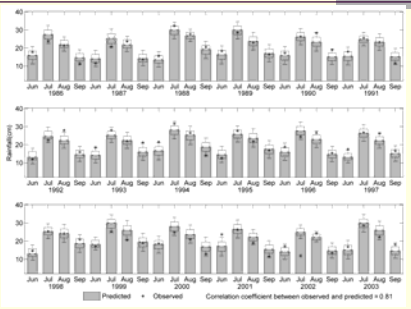

Summary

- A new method is proposed to capture the dependence between the teleconnected hydroclimatic variables for successful prediction of the response variable
- While capturing the relationship, uncertainty associated with the relationship is also provided
- Nonparametric estimates of probability density of the data sets are used in the proposed method
- The proposed method is general in many aspects and can therefore be applied to similar studies irrespective of distributional form, associated uncertainty and nature of dependence.

Monthly Composite Index (MCI) of ENSO and EQUINOO over homogeneous monsoon regions of India

Association of MCI with monthly variation of ISMR considering lagged relationship

Month of			Equation for MCI	Correlation coefficient#
Rainfall anomaly	ENSO	EQUINOO		
Jun	Mar	Mar	$MCI = -0.18 * NINO_{Mar} - 0.29 * EQWIN_{Mar}$	0.38
Jul	Jun	Jun	$MCI = -0.24 * NINO_{Jun} + 0.43 * EQWIN_{Jun}$	0.54
Aug	Jul	Jul	$MCI = -0.24 * NINO_{Jul} + 0.28 * EQWIN_{Jul}$	0.35
Sep	Aug	Jul	$MCI = -0.53 * NINO_{Aug} + 0.44 * EQWIN_{Jul}$	0.65

Coefficients of MCI equations for varied length of data period

$MCI = \alpha \,.\, EN + \beta \,.\, EQ$

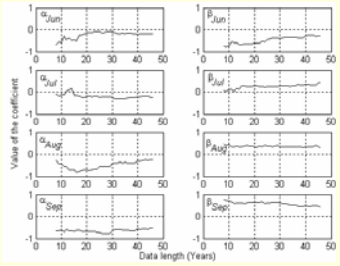

Coefficients of MCI equation for 35 years sliding window

$MCI = \alpha \,.\, EN + \beta \,.\, EQ$

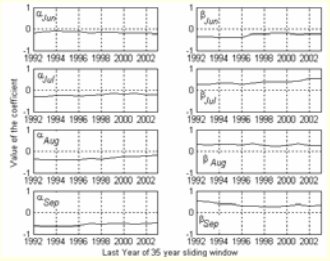

Spatial Variation of Monthly Composite Index and Rainfall*

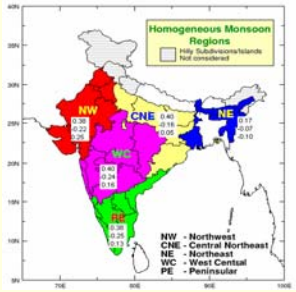

Three different correlation coefficients are shown for each region in a vertical sequence.
These are between the monthly rainfall anomaly during monsoon months and
(1) the MCI,
(2) the ENSO index and
(3) the EQUINOO index, respectively

*** Atmospheric Science Letters, Royal Meteorological Society (RMetS), UK, 2006**

Large-scale circulation phenomena and basin-scale hydrologic variables

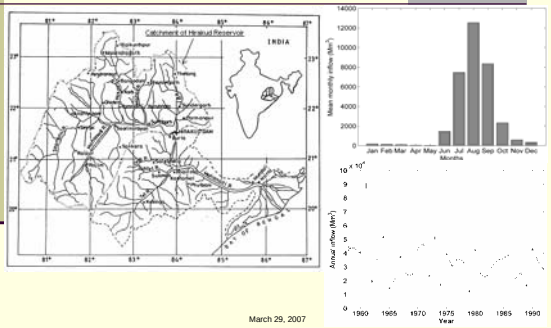

ENSO and Hirakud Inflow

❑ Composite picture of SST anomalies (°C) from Niño 3.4 region for five lowest flow years

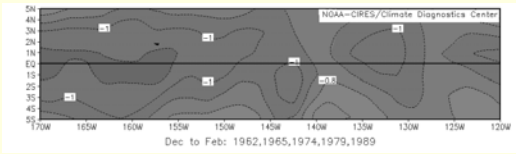

ENSO and Hirakud Inflow

❑ Composite picture of SST anomalies (°C) from Niño 3.4 region for five highest flow years

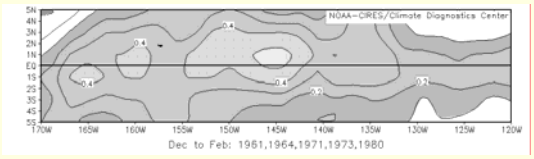

Correlation coefficients

❑ Correlation coefficients of monsoonal inflow into Hirakud reservoir with i) ONI and ii) EQWIN for different premonsoon periods

Period	Correlation Coefficient with ONI	Correlation Coefficient with EQWIN
Dec*, Jan, Feb	0.207	-0.194
Jan, Feb, Mar	0.153	-0.245
Feb, Mar, Apr	0.053	-0.239
Mar, Apr, May	-0.040	-0.077

* Month of previous year

Combined Association

Composite Index $CI = \alpha . EN + \beta . EQ$

By least square technique

$$CI = 0.366\ EN - 0.577\ EQ$$

CI range	NL (CP)	NM (CP)	NH (CP)
< -0.3 (Lower 1/3rd)	5 (0.71)	2 (0.29)	0 (0.0)
-0.3 to 0.3 (Middle 1/3rd)	5 (0.30)	5 (0.30)	7 (0.40)
> 0.3 (Upper 1/3rd)	3 (0.27)	2 (0.18)	6 (0.55)

Prediction of inflow into Hirakud reservoir*

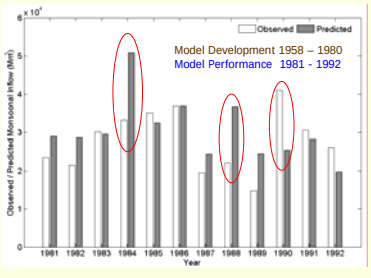

❑ Monsoonal inflow is under-predicted for the year 1990 and over-predicted for the years 1984 and 1988

❑ For the rest of the years, the prediction performance is quite good

*** Journal of Hydrologic Engineering, ASCE, in review**

Sub-basin Map of Mahanadi River

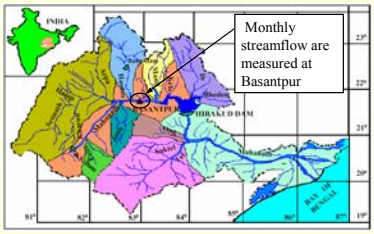

- At monthly time-scale, the hydroclimatic teleconnection between basin-scale streamflow and large-scale atmospheric circulation pattern is more complex.
- Genetic Algorithm based Evolutionary Optimizer is adopted to obtain optimal Artificial Neural Network (ANN) architecture, which is used to capture the complex relationship

GA – ANN Approach

Genetic Algorithm Optimized Artificial Neural Network for Streamflow Prediction with Climate Inputs

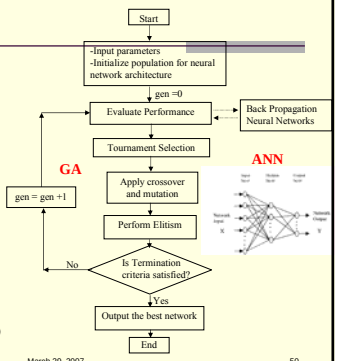

Training Data: 23 years (1958 – 1980)
Testing Data: 10 years (1981 – 1990)

Performance for three different cases@

Month	Considering only streamflow information of previous month(s)			Considering only large-scale atmospheric circulation information			Considering both streamflow (if necessary) and large-scale atmospheric circulation information		
	Inputs*	Best Network	Model Performance#	Inputs*	Best Network	Model Performance#	Inputs*	Best Network	Model Performance#
Jun→	May SF	1-2-2-1	-0.030 833.0 1500.3	Mar EN Mar EQ	2-4-5-3-1	0.542 1209.4 1926.4	Mar EN Mar EQ	2-4-5-3-1	0.542 1209.4 1926.4
Jul→	Jun SF	1-2-2-2	0.731 4312.8 5025.6	Jun EN Jun EQ	2-3-2-1	0.298 5643.6 6059.4	Jun SF Jun EN Jun EQ	3-3-5-1	0.813 3570.9 4425.2
Aug→	Jul SF	1-2-3-1-1	0.412 2929.2 3575.7	Jul EN Jul EQ	2-2-1	0.511 2721.5 3225.6	Jul SF Jul EN Jul EQ	3-6-5-1	0.836 1486.0 2008.5
Sep→	Jul SF Aug SF	2-2-3-1-1	0.321 2331.9 3260.2	Aug EN Aug EQ	2-3-1-2-1	0.402 1877.1 2719.7	Jul SF Aug SF Aug EN Aug EQ	4-3-2-1	0.493 2101.0 2635.6
Oct→	Sep SF	1-2-1	0.838 611.6 761.4	Sep EN Sep EQ	2-4-3-1	0.372 898.8 1228.1	Sep SF Sep EN Sep EQ	3-5-1	0.765 742.2 926.5

Network Performance for Testing Period (1992 – 2003)

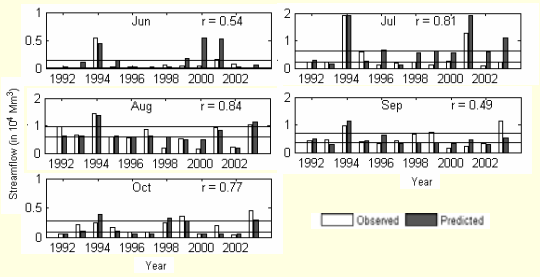

Network Performance for Testing Period (1992 – 2003)

Observed Category of Streamflow	Predicted Category of Streamflow		
	Low	Normal	High
Low	12	6	3
Normal	3	20	4
High	0	3	9

Heidke skill score, $HSS = (CF - CF_{rand})/(N - CF_{rand}) = 0.525$
(Wilks, 2006)

Malaprabha Inflow Forecast Models

Annual Inflow Forecast

$Q_t = f(Nino_{feb}, Nino_{mar}, Q_{t-2}, Q_{t-1})$

Monthly Inflow Forecast

$Q_t = f(Nino_{t-2}, Nino_{t-1}, Q_{t-2}, Q_{t-1})$

Ten-daily inflow Forecast Model

$Q_t = f(Rain_{t-1}, Q_{t-2}, Q_{t-1})$

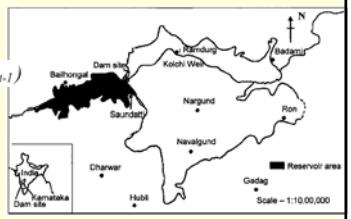

Malaprabha Inflow Forecast Models

Model		Performance measure	PSONN Training	PSONN Validation	PSONN Testing	BPNN Training	BPNN Validation	BPNN Testing	ANFIS Training	ANFIS Validation	ANFIS Testing
Annual	*	*RMSE*	219.6361	309.127	213.7561	234.384	348.4827	292.4613	181.3062	285.7193	271.6191
		MAE	149.8344	268.4584	161.9773	152.4845	306.4618	266.8942	109.9852	232.5193	237.0673
		r	0.9227	0.7575	**0.6327**	0.9185	0.6583	0.5935	0.9516	0.7922	0.6082
		CE	0.8803	0.2165	0.3171	0.8720	0.3256	0.2183	0.9023	0.4325	0.2467
monthly	Monsoon season	*RMSE*	124.2218	88.2118	169.6542	89.5654	98.1284	201.8452	79.0521	74.3287	127.7455
		MAE	72.9947	62.2102	108.9456	64.5592	76.5942	129.9456	45.0099	48.407	90.3816
		r	0.8952	0.8582	0.6632	0.9128	0.65981	0.5962	0.9484	0.9023	**0.6942**
		CE	0.6924	0.7318	0.2313	0.6984	0.5784	0.3384	0.8754	0.8096	0.1834
	Non-monsoon season	*RMSE*	7.5010	6.6121	5.0251	6.8010	7.2121	7.864	4.8216	5.5417	6.9079
		MAE	4.5204	4.7637	3.5612	4.446	5.932	4.9318	3.0864	4.0361	4.1862
		r	0.8814	0.7419	**0.6467**	0.8923	0.5897	0.5863	0.9256	0.8278	0.6213
		CE	0.6299	0.5464	0.4221	0.7639	0.6954	0.32949	0.8471	0.6814	0.409
Ten daily	Monsoon season	*RMSE*	48.1687	55.6173	42.7136	56.5813	62.6837	47.5461	41.1305	53.0554	50.6004
		MAE	27.7492	28.154	24.7922	315873	29.856	26.5829	23.2053	25.0324	28.3243
		r	0.9106	0.7634	**0.6315**	0.8964	0.751	0.6048	0.9296	0.7781	0.5981
		CE	0.692	0.5579	0.3391	0.6234	0.5892	0.3251	0.6494	0.5977	0.3158
	Non-monsoon season	*RMSE*	2.4704	2.5779	2.0503	3.0782	3.8574	2.8569	2.1115	2.158	1.7649
		MAE	1.7180	1.6349	1.5807	2.3351	2.5694	1.6963	1.3777	1.4912	1.4354
		r	0.8915	0.7763	0.6152	0.8625	0.6945	0.5962	0.9126	0.7955	**0.6226**
		CE	0.5328	0.4455	0.2333	0.6482	0.6195	0.2259	0.6587	0.6114	0.4319

Real-time Reservoir Operation*

Real time reservoir operation based on inflow forecasts made using climate inputs

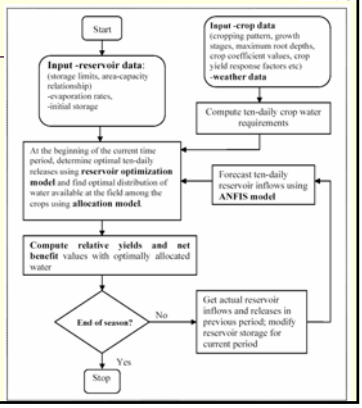

*** Hydrological Processes, Wiley InterScience, in review**

Conclusions

- Bayesian dynamic linear model (BDLM) is newly introduced to the field of hydroclimatology, which is able to capture the time varying dynamic relationship and quantify the uncertainty associated with the predicted values.
- A Copula-based method is able to capture the scale-free dependence pattern and provides a nonparametric way to predict the response variable using the information from causal force.
- Mahanadi River basin is investigated for the basin-scale hydroclimatic teleconnection. Hydroclimatic association at seasonal scale between monsoonal inflow into Hirakud reservoir on Mahanadi River and large-scale circulation phenomena is established.
- At monthly scale, streamflow at Basantpur site in Mahanadi River basin is predicted using GA-ANN approach.
- Inflow forecasts thus obtained are useful for better water resources management.

Thank you